PAPER • **OPEN ACCESS**

On the influence of the refrigerant inlet position and circuitry layout on plate-finned tube evaporator performance through the hybrid method

To cite this article: Silvia Macchitella *et al* 2024 *J. Phys.: Conf. Ser.* **2893** 012091

Journal of Physics: Conference Series **2893** (2024) 012091 doi:10.1088/1742-6596/2893/1/012091

On the influence of the refrigerant inlet position and circuitry layout on plate-finned tube evaporator performance through the hybrid method

Silvia Macchitella[1], Gianpiero Colangelo[1] and Giuseppe Starace[2*]

[1] Dipartimento di Ingegneria dell'Innovazione, Università del Salento, Lecce, Italy
[2] Dipartimento di Ingegneria, Università LUM "Giuseppe Degennaro", Casamassima (Ba), Italy

[*]E-mail: starace@lum.it

Abstract. Multiple factors can impact the performance of a plate-finned tube evaporator in terms of heat transfer rate and refrigerant pressure drops, including the circuitry layout and the position of the refrigerant distributors. In order to assist designers, various circuitry layout alternatives together with different refrigerant inlet positions were examined in this work, using the hybrid method to calculate the evaporator performance. Based on prediction functions coming from the outcomes of either numerical, analytical, or experimental analysis, the hybrid method has the advantage of combining affordable computing costs with accurate findings. Moreover, the refrigerant inlet position can cause uneven vapor quality entering the various circuits. This characteristic, along with the variation in flow rates it implies, was also examined to investigate their influence on the heat exchanger's performance.

1. Introduction

The optimization process of a plate-finned tube heat exchanger (PFTHX) can be very difficult due to the many design variables involved. When compared to other optimization procedures, like altering the fin or tube geometry or the overall dimensions, as discussed by Yun and Lee [1] and Matos et al. [2], optimizing the refrigerant path by modifying circuit arrangement is the best way for cost savings due to limitations that often arise in small installation spaces or dealing with manufacturing issues. Dividing the refrigerant flow over numerous circuits is an efficient way to reduce refrigerant pressure drops and enhance the design. Some authors tested the effects of the refrigerant circuit layout using different circuitry configurations. In a numerical analysis of a fin and tube condenser, Joppolo et al. [3] used the ε-NTU approach to calculate the heat transfer rate between air and refrigerant for each element into which the condenser geometry was divided, accounting for different circuitry layouts. In order to optimize the circuitry arrangement, Wang et al. [4] carried out an experimental investigation on different circuitry topologies on wavy fin condensers, taking refrigerant pressure losses into consideration. The counter-cross arrangement provided the best performance.

Other authors focused on circuit optimization through intelligent systems studies and developed simulation tools or genetic algorithms (GA) that considered variables such as heat exchanger capacity maximum [5,6,7,8,9], minimum heat transfer surface value with the same heat transfer rate [8,9], and minimum entropy generation [10,11]. Nevertheless, these studies neglect to investigate at how circuitry design affects pressure drop, which helps reduce operational costs. An integer permutation-based genetic algorithm (IPGA) was developed by Li

et al. [12] for circuit optimization under operational and manufacturability constraints. Every chromosome produced by IPGA can be sorted using the genetic operators in a functional circuit structure. As a result, this method may more successfully search the solution space than traditional GA.

Before proceeding to the optimization of the circuits, a fundamental choice the designer must make is the selection of the model to be used for calculating the performance of the heat exchanger. Models can be classified as small, large, or multi-scale by applying a distinct scale technique [13]. Computational fluid dynamics (CFD) approaches analyse small-scale interaction events in great detail, therefore their conclusions are often very accurate. On the other hand, they are often expensive in terms of time and costs. Accurate small-scale studies that focus on fin profiles and tube geometries can be found in [14-20]. On the other hand, large-scale approach models are very helpful for manufacturing companies as they are simpler and quicker to deploy. Typically, these are analytical models that are often developed through experimentation. The disadvantage of these models is that sometimes they can produce somewhat inaccurate findings. It is the most commonly used approach for calculating performance, as evidenced by numerous studies in the literature [21-26]. Multi-scale models are very flexible and suitable for different HX geometries and working conditions because they integrate analytical methods' benefits with more precise numerical approaches.

Developed by Starace et al. [27], the hybrid technique is an alternative design process based on an algorithm that applies a multi-scale strategy based on data from either analytical, numerical, or experimental research. Initially, the hybrid technique was applied to compact cross-flow HXs, in which the whole geometry was divided into many control volumes, each having a warm and a cold side. The prediction functions of heat transfer were developed by applying a regression technique to the thermo-fluid dynamics simulation results on the two finned surfaces of the HXs by Carluccio et al. [28]. This extended the local results over the entire geometry of the HX. Fiorentino and Starace [29] created a different use of the hybrid technique for countercurrent evaporative condensers to evaluate their performance by starting with experimental studies. Then, utilizing the control volume approach, Starace et al. [30] applied this technique to a plate-finned evaporator with a simple refrigerant circuit layout. Starace et al. [31] made advancements in the hybrid technique by applying it to evaporators with elaborate circuit layouts to evaluate how circuitry configuration affects overall performance. The findings show that when the number of circuits increases, the heat transfer rate as well as pressure losses lowers considerably; hence, installation costs will increase while operating costs will fall. Later, more experiments were carried out while varying the fluid conditions at the input and accounting for different refrigerants [32–33]. The results of additional research on various circuitry layouts indicate that the performance of the HX's heat transfer rate is not significantly affected by the air inlet side [32].

In this paper the hybrid method is used to further investigate on the impact of refrigerant entry position and circuitry layout on the heat exchanger (HX) performance in terms of heat transfer rate and refrigerant pressure drops. Additionally, some simulations were conducted considering the non-uniform refrigerant vapor quality at the inlet of each circuit, which can occur due to the different entry positions into the various circuits within the distribution manifold, as well as the resulting flow rate distribution.

2. Mathematical model

The model uses a three-dimensional matrix to identify each of the tube-centered elementary cells that make up the HX's overall architecture (Figure 1).
The case study's heat exchanger is a staggered finned tube exchanger with refrigerant as working fluid that evaporates due to the heat exchange occurring with the air flowing perpendicularly to the tubes between the fins. The evaporator is made up of two or more intricate circuits that have the same number of pipes in each and through which the refrigerant flows. The bends joining the pipes are disregarded throughout the heat transfer process.

The following is a list of the assumptions that guide the mathematical model:

- Frost formation is not modelled. Anyway, it was verified that in all the simulation cases that were conducted, there is no frost formation;
- the refrigerant fluid never reaches superheated vapor condition;
- calculations are performed in steady-state;
- all parameters are considered constant within each elementary cell into which the evaporator is divided;
- the pipe junction bends are excluded from the heat transfer process.

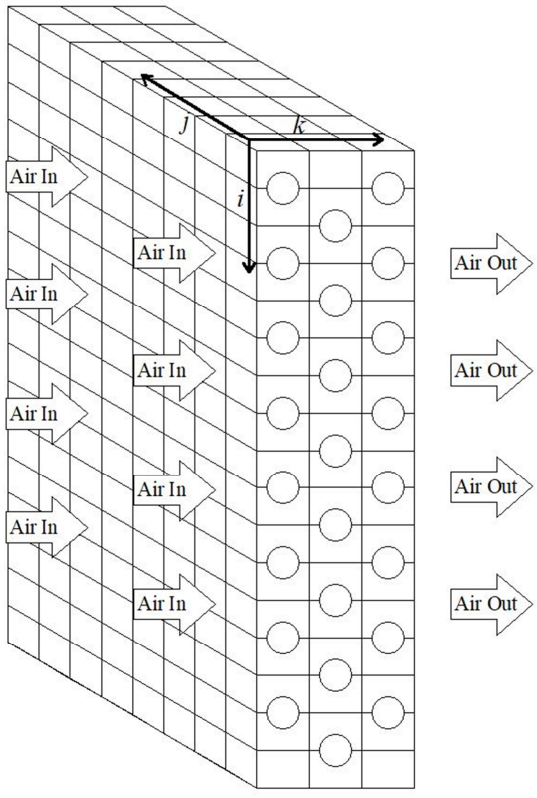

Figure 1. Evaporator representation through a three-dimensional matrix.

In the staggered pipes of the evaporator, an edge cell with no pipes is placed at the top of each row of even numbers and at the bottom of each row of odd numbers. Each border cell's attributes are computed separately. The following input data are needed for the iterative computation of the heat transfer rate and wall temperature for all the other cells:

- the HX geometrical configuration;
- refrigerant circuitry arrangement;
- the operating conditions;
- the regression coefficients, which are obtained by applying the results of experimental, numerical, or analytical research.

Scanning the matrix cells one after another in order to perform the calculation, the algorithm assigns to each cell the refrigerant flow rate and the vapor quality that corresponds to the circuit under consideration after determining the refrigerant flow direction, the circuit to which the tube belongs, and the branch tube (i.e. the previous tube in the refrigerant flow order) (Figure 2). In the initial delivery cell of every circuit, the vapor quality and flow rate are set equal to the input parameters. Assuming that the bends are adiabatic, the method assigns the same refrigerant properties at the branch pipe's output for all consecutive cells.

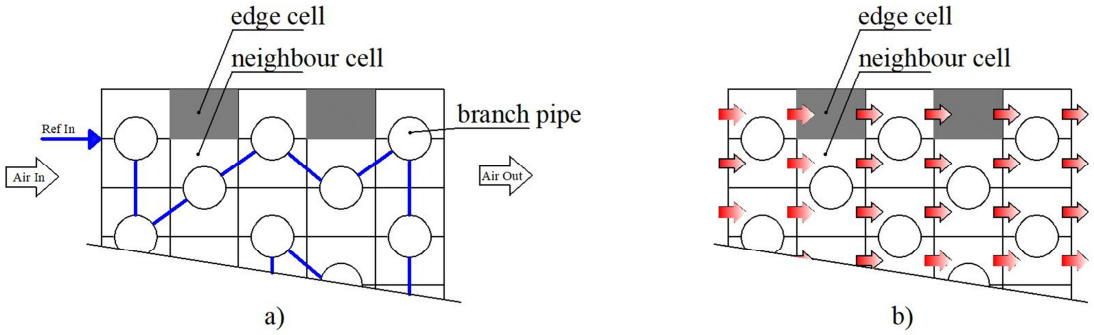

Figure 2. Schematic representation of refrigerant (a) and air (b) path.

For each cell, the algorithm determines the tube wall temperature through an iterative calculation until the convergence condition expressed in the Equation (1) is satisfied: the air-side heat transfer rate must equal the refrigerant-side heat transfer rate, considering the convective contribution of the air and refrigerant and the conductive contribution of the tube.

$$\dot{Q}_R = \dot{Q}_A \tag{1}$$

With the aid of a quadratic regression technique, the prediction function for computing the thermal power and all other thermodynamic parameters is extrapolated in an effort to determine the correlation between the input and output variables on the air and refrigerant sides. The data for the regression technique in this case study came from the experimental correlations displayed in Table 1, but because of the model's high degree of adaptability, it is also possible to use the results of numerical analysis as well as of experimental tests when available.

The refrigerant side response variable $x_{R,out}$ is derived using Equation (2), whereas the air side response variables $T_{A,out}$, $i_{A,out}$, and $p_{A,out}$ are determined using Equation (3).

$$\beta \cdot \gamma^T \tag{2}$$

$$\beta \cdot \alpha^T \tag{3}$$

where the vector β contains the 15 polynomial coefficients that were obtained from the regression analysis, and the vectors whose elements are shown in Table 2 are α and γ, respectively.

Table 1. Correlations used for air side and refrigerant side variables computing.

Air side	Reference	Refrigerant side	Reference
Heat transfer coefficient	[34]	Total heat transfer	[40][41]
Lewis number	[35]	Pressure drop	[42]
Overall fin efficiency	[36]		
Pressure drop	[37]		
Air specific humidity	[38]		
Friction factor	[39]		

Table 2. Elements of vectors α and γ.

Element	Value	Element	Value	Element	Value	Element	Value	Element	Value	Element	Value
α_0	1	α_5	$G_R\, x_{R,in}$	α_{11}	$T_R T_{w,i}$	γ_0	1	γ_5	$T_{A,in}RH_{A,in}$	γ_{11}	$V_{A,in}T_{w,o}$
α_1	G_R	α_6	$G_R T_{w,i}$	α_{12}	G_R^2	γ_1	$T_{A,in}$	γ_6	$T_{A,in}V_{A,in}$	γ_{12}	$T_{A,in}^2$
α_2	$x_{R,in}$	α_7	$G_R T_R$	α_{13}	$x_{R,in}^2$	γ_2	$RH_{A,in}$	γ_7	$T_{A,in}T_{w,o}$	γ_{13}	$RH_{A,in}^2$
α_3	$T_{w,i}$	α_8	$x_{R,in}T_{w,i}$	α_{14}	$T_{w,i}^2$	γ_3	$V_{A,in}$	γ_8	$RH_{A,in}V_{A,in}$	γ_{14}	$V_{A,in}^2$
α_4	T_R	α_9	$x_{R,in}T_R$	α_{15}	T_R^2	γ_4	$T_{w,o}$	γ_9	$RH_{A,in}T_{w,o}$	γ_{15}	$T_{w,o}^2$

Rather than being determined by the convergence approach, the edge cell's heat transfer rates are computed as a percentage of the heat transfer rates of the neighbouring cells, which are located below the edge cell in odd ranks and above in even ranks Figure 2. After calculating all of the cells as per Equation (4), the algorithm checks pressure drops on the air-side and refrigerant-side. The air mass flow rate is then redistributed into each cell once more by the algorithm, altering the flow rate in accordance with the error from the mean value if the condition in Equation (5) is not met. The pressure drops for every refrigerant circuit should be within 1% of the mean value, as per Equation (6). After then, the program divides up the refrigerant flow rates among the circuits until the condition of every z-th circuit is verified.

$$\Delta p_A(i,j) = \sum_{k=1}^{N_k} \Delta p_A(i,j,k) \tag{4}$$

$$\Delta p_A(i,j) = \Delta p_{A,m} \tag{5}$$

$$\Delta p_{R,z} = \Delta p_{R,m} \tag{6}$$

3. Setup of simulation case studies

Three different simulation tests were conducted with the aim to investigate the influence of refrigerant inlet position and circuitry layout on a plate-finned tube evaporator performance using the hybrid method algorithm. Figure 3 shows the 4 circuitry layouts that were used for the simulations, each of which has different characteristics. Layouts A, B, and C consist of 5 circuits each, but the inlet position to the various circuits is different for the three layouts. Layout A has the inlet positions evenly distributed along the entire height of the battery; layout B has the

inlets at the top and bottom of the battery, while configuration C has the inlets in the central part of the battery. Configuration D, on the other hand, has 10 circuits with the inlet distributed along the entire battery. All configurations are based on an evaporator consisting of 3 rows, with each circuit comprising 12 tubes for layouts A and B, and 6 tubes each for layout C.

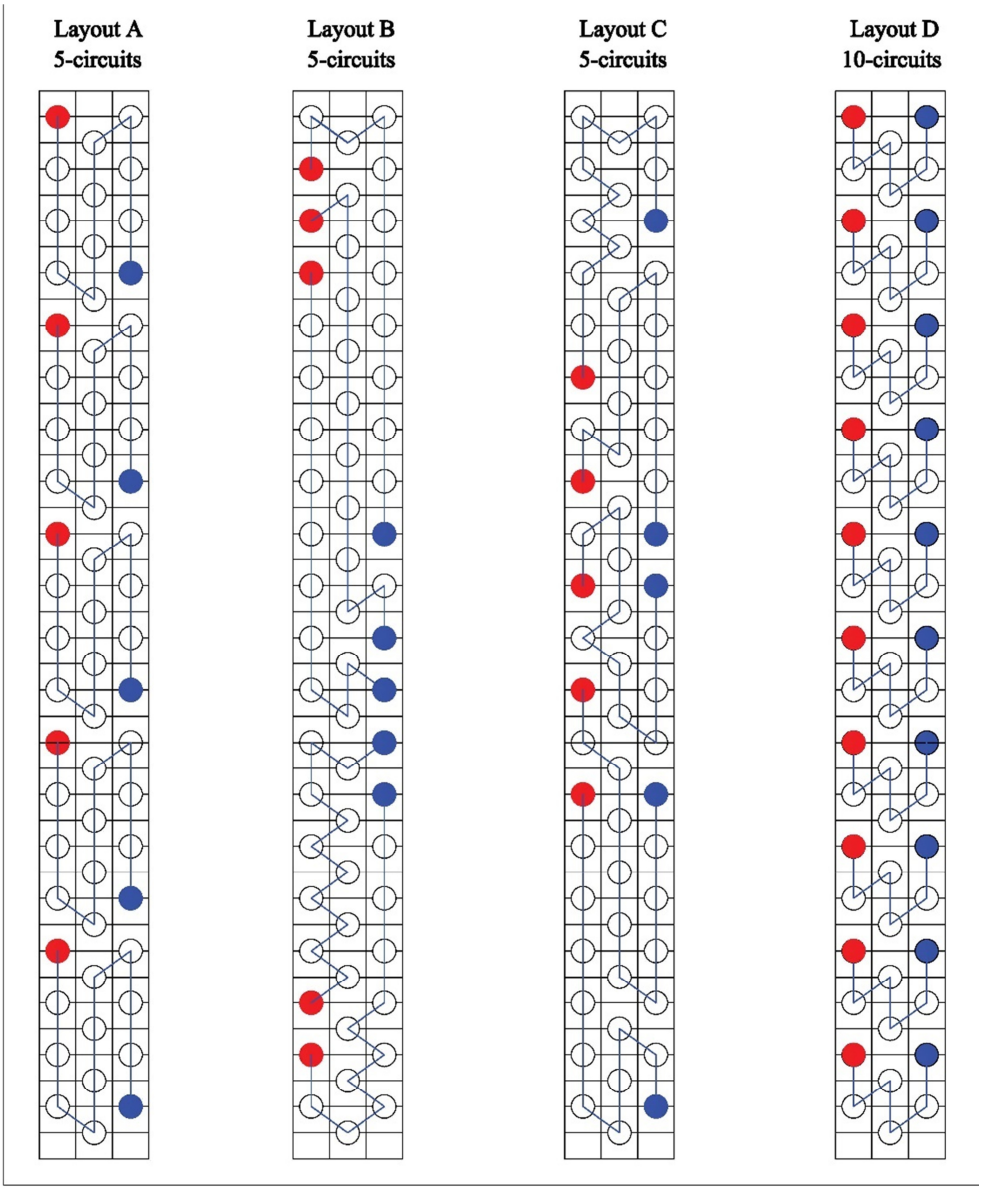

Figure 3. Circuitry layouts used for simulation tests. The blue line represents the path of the refrigerant through the tubes. The red and blue dots represent the inlet and outlet tubes for each circuit, respectively.

Each of the three simulation tests that were performed had a clear aim, as stated below:

- Test no.1: performance comparison between layout A and layout D that have the same number of tubes in total but different number of refrigerant circuits.
- Test no.2: performance comparison between layouts A, B and C that have the same number of refrigerant circuits but different inlet positioning and so different circuit arrangements, with uniform refrigerant vapor quality at the inlet of each circuit.

- Test no.3: performance comparison between layouts A, B and C with non-uniform refrigerant vapor quality at the inlet of each circuit.

4. Results and discussion

In this section the outcomes of applying the hybrid method to a 3-row evaporator with different circuit layouts in terms of refrigerant pressure drops and heat transfer rate will be discussed. Three tests were carried out on four circuitry configurations with the intention of supporting designers in their decision-making process, by varying:

- the number of refrigerant circuits and refrigerant fluid (test no.1)
- circuitry arrangement and refrigerant inlet positions for each circuit, with uniform vapor quality at inlet for each circuit (test no.2)
- circuitry arrangement and refrigerant inlet positions for each circuit, with non-uniform vapor quality at inlet for each circuit (test no.3)

The operating condition are indicated in Table 3 while the evaporator characteristics are summarized in Table 4.

Table 3. Simulation setup for test no.1, test no.2 and test no.3.

Quantity	**Unit**	**Test no.1**	**Test no.2**	**Test no.3**
Refrigerant fluid	-	R32/R134a/R410a	R32	R32
Number of tubes per row	-	20	20	20
Refrigerant mass flow rate	kg/s	0.058	0.058	0.058
Air mass flow rate	kg/s	1.24	1.24	1.24
Evaporation temperature	K	270.5	271.5	271.5
Air inlet temperature	K	288	288	288
Air inlet relative humidity	-	0.65	0.65	0.65
Inlet vapor quality	-	0	0	Layout A: 0.4/0.4/0/0/0 Layout B: 0.4/0.4/0.4/0/0 Layout C: 0.4/0.4/0/0/0
Air inlet velocity	m/s	4	4	4

The purpose of test no. 1 was to compare the performance in terms of heat transfer rate and refrigerant pressure drops between layout A and layout D, which, while having the same evaporator size, have a different number of circuits. The comparison between different circuit layouts had already been addressed by the same authors in [31]. However, the coil used for those simulations was smaller. Therefore, to confirm the results of the previous simulations and validate the model with a larger coil (12 tubes per row vs. 20 tubes per row), test no. 1 was carried out, also with different refrigerants (R32, R134a, R410a). Results in Figure 4 confirmed what was already assessed: when the number of circuits increases, heat transfer rate decreases as well as the refrigerant pressure drops, also with a bigger coil. In detail, heat transfer rate reduces of 7.8% as a mean among the refrigerants passing from a 5-circuits layout to a 10-

circuits layout, while, on the other hand, pressure drops have a mean strong reduction of 66% with layout D with respect to layout A. Increasing the number of circuits causes a drop in the refrigerant flow rate across each circuit, which in turn causes a fall in the convective heat transfer coefficient. This has a negative effect on the overall heat transfer.

All the simulated refrigerants exhibited the same trend, confirming that the model is able to predict the evaporator performance with different refrigerants. In particular, R32 shows the best overall performance: it has a higher heat transfer rate with relatively low pressure drops, due to the typical properties of this refrigerant.

Table 4. Geometric characteristics of simulated evaporator.

Tubes			**Fins**		
Quantity	**Unit**	**Value**	**Quantity**	**Unit**	**Value**
Material	-	Copper	Material	-	Aluminum
Internal diameter	mm	7.38	Thickness	mm	0.1
External diameter	mm	7.94	Pitch	mm	2
Length	mm	500			
Longitudinal pitch	mm	21.65			
Transversal pitch	mm	25			

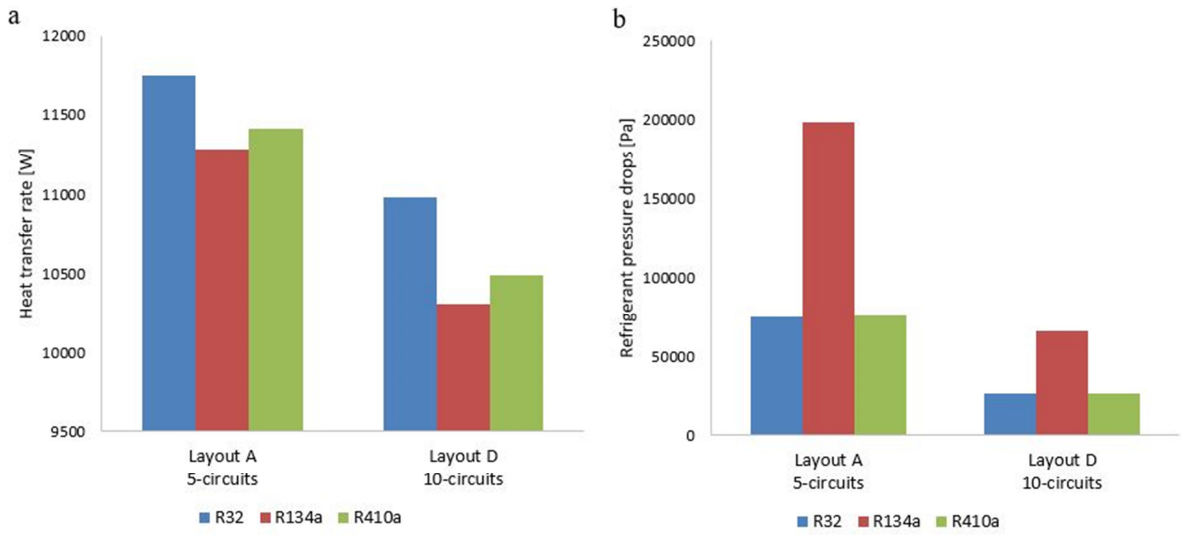

Figure 4. Test no.1 a): heat transfer rate and b) refrigerant pressure drops for layout A and layout D. Tested refrigerants: R32, R134a, R410a.

The goal of tests no.2 and test no.3 was to optimize the circuitry arrangement maintaining the same number of circuits for the best performance in terms of transferred heat between air and refrigerant (R32) and pressure losses which is known to have a strong impact on operational costs. In particular, the three 5-circuits layouts (Layout A, B and C) considered for comparison,

present different entry positions for each circuit and consequently different circuit arrangement. Moreover, the circuit inlet position can influence the inlet vapor quality at each circuit. For this reason, both tests were conducted on the same layouts but with the circuit vapor quality at inlet all the same for test no.2 and with non-uniform inlet vapor quality for each circuit for test no.3. Results in Figure 5 for test no.2 show that given the same number of circuits, layout A is quite similar to layout B in terms of heat exchange power (+0.33% of layout A compared to layout B for test no. 2), while layout B has the lowest pressure drops (-1.7% compared to layout A for test no. 2). On the contrary, in test no. 3 with non-uniform vapor qualities, layout B shows almost equal heat transfer rate with respect to the other layouts (+0.8% compared to layout C) but also higher pressure drops, which are lower with layout C (-10.2% of layout C compared to B in terms of pressure drops). This happens because, in the case of non-uniform inlet vapor qualities, the flow rates to the circuits must also be non-uniform to maintain equal pressure drops across the circuits, as shown in the graphs in Figure 6 (d), Figure 6 (e) and Figure 6 (f). The circuits with higher inlet qualities (circuit 1 and circuit 2 for layouts A and C; circuits 1, 2, and 3 for layout B) also have higher flow rates and therefore higher pressure drops. Conversely, in test no. 2, the inlet vapor qualities are uniform and the distribution of flow rates to the circuits is balanced as well, as shown in the graphs in Figure 6(a), Figure 6(b) and Figure 6(c).

Therefore, test no.2 and test no.3 show that optimizing the layout while maintaining the same number of circuits is possible, but the benefits in terms of heat transfer rate and pressure drops are limited, if we consider ideal refrigerant inlet conditions, such as uniform inlet qualities to all circuits. On the other hand, when considering non-uniform vapor qualities, the influence of the circuitry arrangement is more evident, especially in terms of pressure drops due to a non-uniform distribution of flow rates between the circuits. Therefore, designers need to make a trade-off between these benefits and the optimization costs during the development phase.

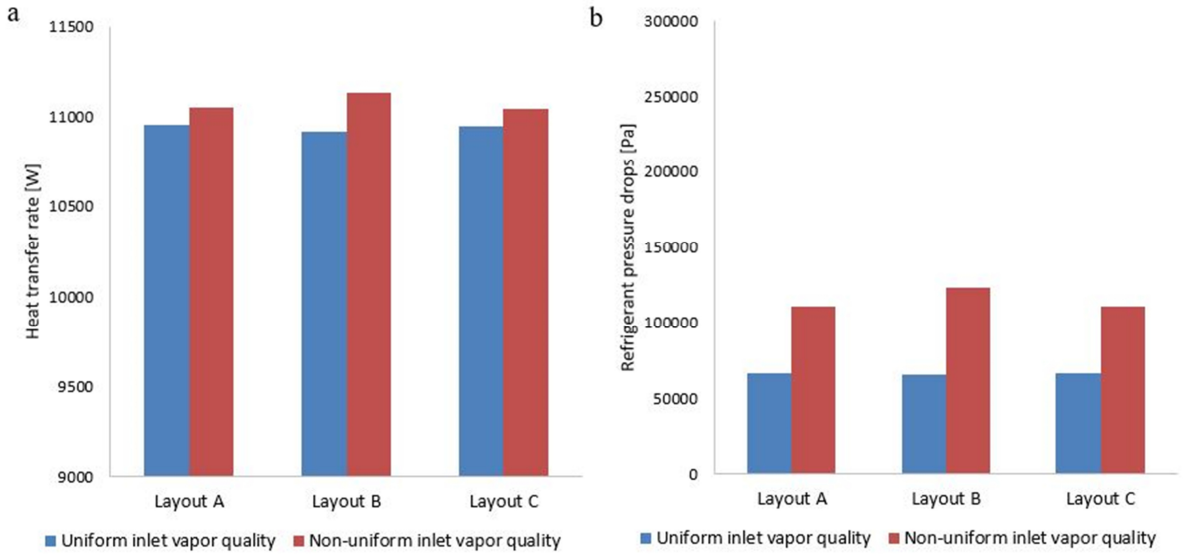

Figure 5. a) Heat transfer rate and b) Refrigerant pressure drops for test no.2 (uniform inlet vapor quality) and test no.3 (non-uniform inlet vapor quality) on layout A, layout B and layout C.

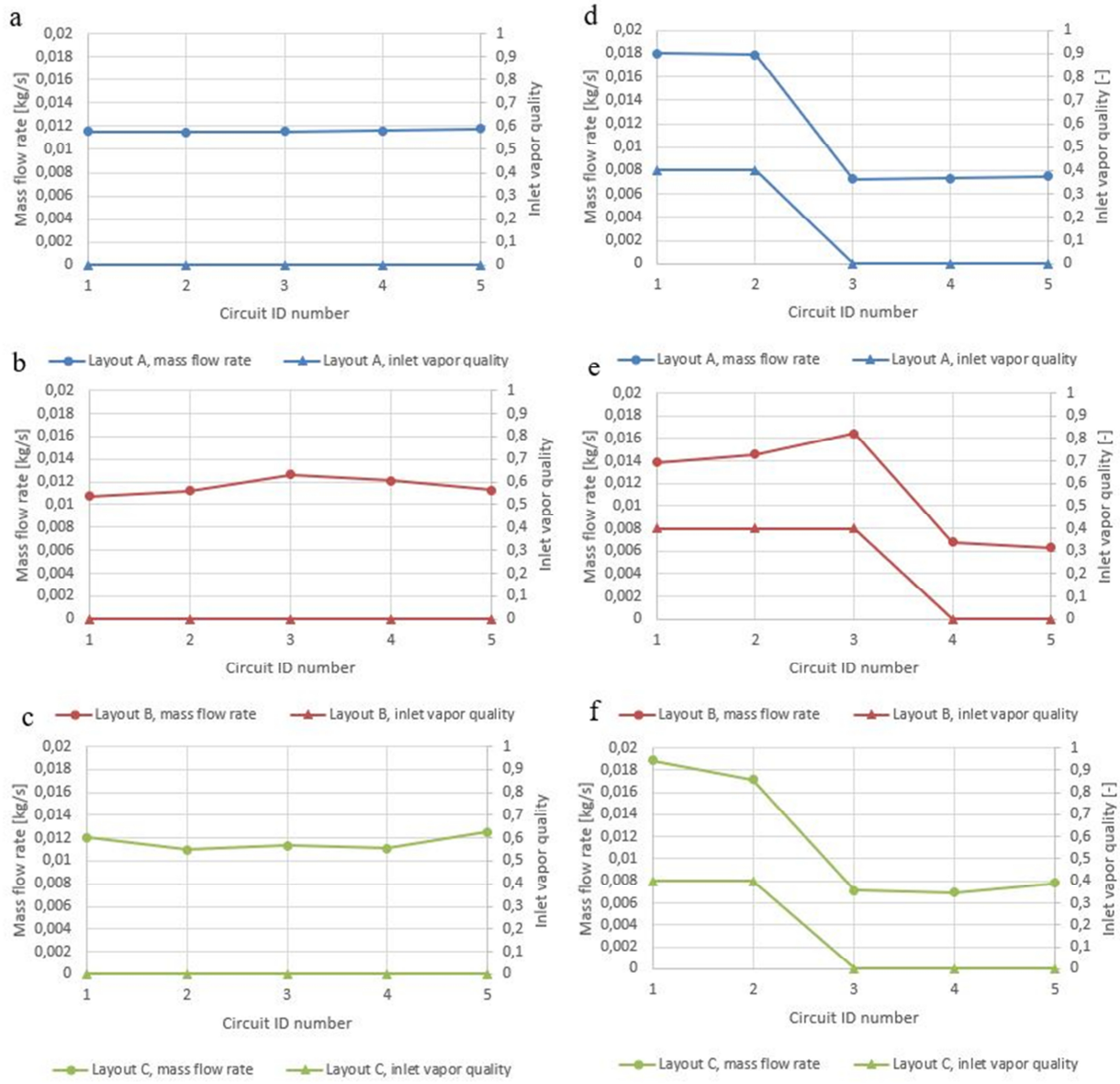

Figure 6. Refrigerant mass flow rate and vapor quality for each circuit of layout A (a), layout B (b) and layout C (c) for uniform vapor quality at inlet and of layout A (d), layout B (e), layout C (f) for non-uniform vapor quality at inlet.

In order to optimize the circuit arrangement, a very useful tool for the designer could be to analyse in detail the thermal power for each circuit and for each tube section along the refrigerant path, by creating graphs like in Figure 7. In layout A (Figure 7(a)), it can be seen that the less performing circuits are circuits 2, 3, and 4, while in layout B (Figure 7(b)), circuit 1 could still be optimized. Again, from Figure 7(c), it can be seen that circuits 2 and 4 have lower heat exchange power compared to the other circuits. This type of analysis allows the designer to identify the critical points of the coil and so its areas for improvement.

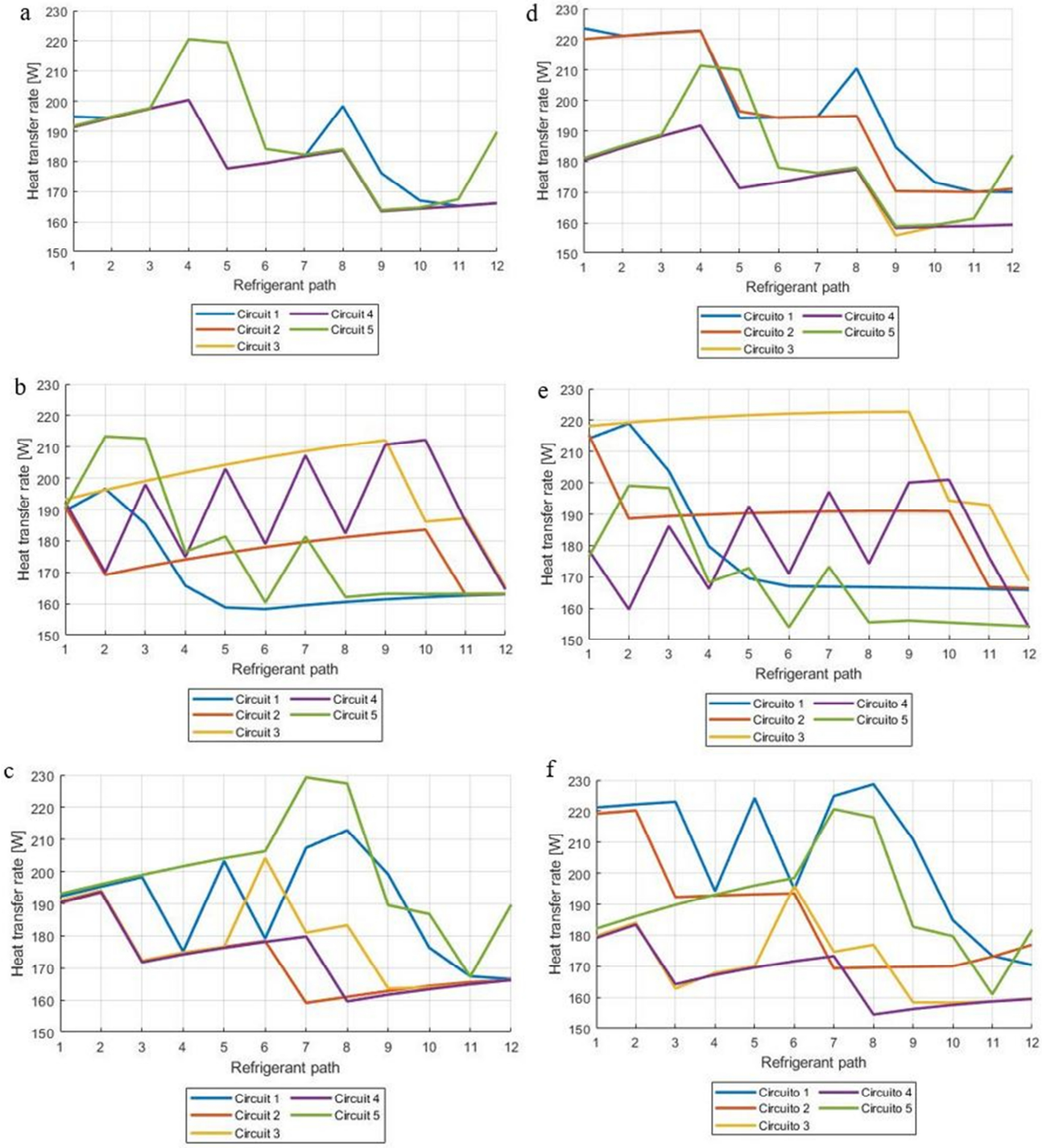

Figure 7. Heat transfer rate vs. refrigerant path for each circuit of layout A (a), layout B (b) and layout C (c) for uniform vapor quality at inlet and of layout A (d), layout B (e), layout C (f) for non-uniform vapor quality at inlet.

5. Conclusions

A multi-scale model already known as the hybrid method, which performs a local analysis to acquire the heat transfer characteristics on each elementary volume, was built in order to compare different circuitry layouts and give designers useful information for the design process of plate-finned tube heat exchangers. Here, the prediction functions were identified by using the regression technique on data from experimental correlations from literature. These prediction functions were then used to determine the air and refrigerant side thermodynamic properties. The advantage of this method is its high flexibility because it allows the use of data from both numerical or analytical analyses, obtaining fairly accurate results at low costs.

Four different circuit layouts were developed and used to run three different simulation tests. The results showed that for all the tested refrigerants (R32, R410a, R134a), the heat transfer rate decreases as the number of circuits increases (-7.8%), and pressure drops decrease drastically when the number of circuits increases (-66%). Among refrigerants, R32 exhibited the best overall performance: it has a higher heat transfer rate with relatively low pressure drops. Additional tests were then conducted on three different layouts with the same number of circuits but different refrigerant entry positions to optimize their performance. The simulation conducted with uniform inlet vapor qualities to the circuits revealed that an optimization is possible, but the improvement in terms of increased heat transfer rate or decreased refrigerant pressure drop is minimal (+0.33% for heat transfer rate, -1.7% for pressure drops). Therefore, it could be concluded that the inlet position of the various circuits in the distribution manifold and consequently the circuitry layout have minimal influence. However, when considering the case of the simulation conducted on the same layouts but with non-uniform inlet vapor qualities, the circuit arrangement can have a greater influence, especially in terms of pressure drop (-10.2% for best layout). This happens because, with constant pressure drops across the various circuits, the flow rates to the circuits are non-uniform, as are the inlet vapor qualities. For this reason, the same authors will aim in the future to test more configurations under real conditions, such as non-uniform intake air as an operating condition, modelling frost formation, and continuously adding more features to the hybrid method model to make it more representative of the actual operation of a coil. Providing these tools to designers is extremely important to avoid over- or under-sizing and consequently wasting resources both during construction and in operating conditions.

Nomenclature

G	mass flux (kg m-2 s-1)
Δp	pressure drop (Pa)
Q	heat transfer rate (W)
RH	relative humudity
T	temperature (K)
V	velocity (m s-1)
x	vapor quality

Greek symbols

β	regression coefficient

Subscripts

A,R	air, refrigerant
in	inlet
m	mean value
o	outer
out	outlet
w	wall

Abbreviations

HX	heat exchanger
PFTHX	Plate-finned tube heat exchanger

References

[1] Yun, J.Y.; Lee, K.S. Influence of design parameters on the heat transfer and flow friction characteristics of the heat exchanger with slit fins. Int. J. Heat Mass Transf. 2000, 43, 2529–2539.
[2] Matos, R.S.; Laursen, T.A.; Vargas, J.V.C.; Bejan, A. Three-dimensional optimization of staggered finned circular and elliptic tubes in forced convection. Int. J. Therm. Sci. 2004, 43, 477–487.
[3] Joppolo, C.M.; Molinaroli, L.; Pasini, A. Numerical analysis of the influence of circuit arrangement on a fin-and-tube condenser performance. *Case Stud. Therm. Eng.* **2015**, *6*, 136–146.
[4] Wang, C.-C.; Jang, J.-Y.; Lai, C.-C.; Chang, Y.-J. Effect of circuit arrangement on the performance of air-cooled condensers. *Int. J. Refrig.* **1999**, *22*, 275–282.
[5] Domanski, P.A.; Yashar, D. Optimization of finned-tube condensers using an intelligent system. Int. J. Refrig. 2007, 30, 482–488.
[6] Domanski, P.A.; Yashar, D.; Kaufman, K.A.; Michalski, R.S. An optimized design of finned-tube evaporators using the learnable evolution model. HVACR Res. 2004, 10, 201–211.
[7] Yashar, D.; Wojtusiak, J.; Kaufman, K.; Domanski. P.A. A dual-mode evolutionary algorithm for designing optimized refrigerant circuitries for finned-tube heat exchangers. HVACR Res. 2012, 18, 834–844.
[8] Wu, Z.; Ding, G.; Wang, K.; Fukaya, M. Application of a genetic algorithm to optimize the refrigerant circuit of fin-and-tube heat exchangers for maximum heat transfer or shortest tube. Int. J. Therm. Sci. 2008, 47, 985–997.
[9] Wu, Z.; Ding, G.; Wang, K.; Fukaya, M. Knowledge-based evolution method for optimizing refrigerant circuitry of fin-and tube heat exchangers. HVACR Res. 2008, 14, 435–452.
[10] Ye, H.-Y.; Lee, K.-S. Refrigerant circuitry design of fin-and-tube condenser based on entropy generation minimization. Int. J. Refrig. 2012, 35, 1430–1438.
[11] Lee, W.-J.; Kim, H.J.; Jeong, J.H. Method for determining the optimum number of circuits for a fin-tube condenser in a heat pump. Int. J. Heat Mass Transf. 2016, 98, 462–471.
[12] Li, Z.; Aute, V.; Ling, J. Tube-fin heat exchanger circuitry optimization using integer permutation based Genetic Algorithm. *Int. J. Refrig.* **2019**, *103*, 135–144.
[13] Macchitella, S.; Colangelo, G.; Starace, G. Performance Prediction of Plate-Finned Tube Heat Exchangers for Refrigeration: A Review on Modeling and Optimization Methods. *Energies* **2023**, *16*, 1948.
[14] Bhuiyan, A.A.; Islam, A.S. CFD analysis of different fin-and-tube heat exchangers. *J. Mech. Eng.* **2011**, *62*, 237-249.
[15] Lee, Y.T.; Chien, L.H.; He, J.; Wen, C.-Y.; Yang, A.S. Air side performance characterization of wavy Fin-and-tube heat exchangers having elliptic tubes with large waffle heights. *Appl. Therm. Eng.* **2022**, *217*, 119220.
[16] Rauber, W.K.; Silva, U.F.; Vaz, M.; Alves, M.V.C.; Zdanski, P.S.B. Investigation of the effects of fin perforations on the thermal-hydraulic performance of Plate-Finned heat exchangers. *Int. J. Heat Mass Transf.* **2022**, *187*, 122561.
[17] Li, Y.; Qian, Z.; Wang, Q. Numerical investigation of thermohydraulic performance on wake region in finned tube heat exchanger with section-streamlined tube. *Case Stud. Therm. Eng.* **2022**, *33*, 101898.
[18] Lindqvist, K.; Skaugen, G.; Meyer, O.H.H. Plate fin-and-tube heat exchanger computational fluid dynamics model. *Appl. Therm. Eng.* **2021**, *189*, 116669.
[19] Taler, D.; Taler, J.; Trojan, M. Thermal calculations of plate-fin-and-tube heat exchangers with different heat transfer coefficients on each tube row. *Energy* **2020**, *203*, 117806.
[20] Taler, D.; Taler, J.; Wrona, K. Transient response of a plate-fin-and-tube heat exchanger considering different heat transfer coefficients in individual tube rows. *Energy* **2020**, *195*, 117023.
[21] Kays, W.M.; London, A.L. *Compact Heat Exchangers*, 3rd ed.; McGraw-Hill: New York, NY, USA, 1984.
[22] Corberan, J.M.; Garcia, M. Modelling of plate finned tube evaporators and condensers working with R134a. *Int. J. Refrig.* **1998**, *21*, 273-284.
[23] Jiang, H.; Aute, V.; Radermacher, R. CoilDesigner: A general-purpose simulation and design tool for air-to-refrigerant heat exchangers. *Int. J. Refrig.* **2006**, 29, 601-610.
[24] Tarrad, A.H.; Al-Nadawi, A.K. Modelling of finned-tube using pure and zeotropic blend refrigerants. In Proceedings of the ATINER' S Conference, Athens, Greece, 17-20 December 2015.
[25] Tong, L.; Li, H.; Wang, L.; Sun, X.; Xie, Y. The effect of evaporator operating parameters on the flow patterns inside horizontal pipes. *J. Therm. Sci.* **2011**, *20*, 324-331.
[26] Domanski, P.A. Finned-tube evaporator model with a visual interface. In Proceedings of the International Congress of Refrigeration 20th. IIR/IIF, Sydney, Australia, 19-24 September 1999.

[27] Starace, G.; Fiorentino, M.; Longo, M.P.; Carluccio, E. A hybrid method for the cross flow compact heat exchangers design. *Appl. Therm. Eng.* **2017**, 111, 1129–1142.
[28] Carluccio, E.; Starace, G.; Ficarella, A.; Laforgia, D.; Numerical analysis of a cross-flow compact heat exchanger for vehicle applications. *Appl. Therm. Eng.* **2005**, 25, 1995–2013.
[29] Fiorentino, M.; Starace, G. The design of countercurrent evaporative condensers with the hybrid method. *Appl. Therm. Eng.* **2018**, 130, 889–898.
[30] Starace, G.; Fiorentino, M.; Meleleo, B.; Risolo, C. The hybrid method applied to the plate-finned tube evaporator geometry. *Int. J. Refrig.* **2018**, 88, 67–77.
[31] Starace, G.; Macchitella, S.; Fiorentino, M.; Colangelo, G. Influence of circuit arrangement on evaporator performance using the hybrid method. In Proceedings of the 6th IIR Conference on Thermophysical Properties and Transfer Processes of Refrigerants, Vicenza, Italy, 1–3 September 2021.
[32] Starace, G.; Macchitella, S.; Colangelo, G. The hybrid method for the plate-finned tube evaporator design process. In Proceedings of the 76° ATI Conference, Rome, Italy, 15–17 September 2021.
[33] Starace, G.; Macchitella, S.; Colangelo, G. Improvements to the hybrid method applied to the design of plate-finned tube evaporators. In Proceedings of the 77° ATI Conference, Bari, Italy, 12–14 September 2022.
[34] Bourabaa, A.; Saighi, M.; Belal, I. The influence of the inlet conditions on the air side heat transfer performance of plain finned evaporator Int. J. Math. Comput. Phys. Elect. Comput. Eng. **2011**, 5 (11) 1667–1670.
[35] Wang, C.C.; Lin, Y.T.; Lee, C.J. An airside correlation for plain fin-and-tube heat exchangers in wet conditions Int. J. Heat Mass Transf. **2000**, 43 (10) 1869–1872.
[36] Thulukkanam, K. Heat Exchanger Design Handbook (CRC Press) **2013.**
[37] Kays, W.M.; London, A.L. Compact Heat Exchanger third ed. (McGraw-Hill, New York) **1984.**
[38] Ma, X.; Dinga, G.; Zhanga, Y.; Wang, K. Airside heat transfer and friction characteristics for enhanced fin-and-tube heat exchanger with hydrophilic coating under wet conditions Int. J. Refrigeration **2007,** 30 (7) 1153–1167
[39] Liang, S.Y.; Wong, T.N. Experimental validation of model predictions on evaporator coils with an emphasis on fin efficiency Int. J. Therm. Sci. **2010**, 49 187–195.
[40] Choi, T.Y.; Kim, Y.J.; Kim, M.S.; Ro, S.T. Evaporation heat transfer of R-32, R-134a, R-32/134a and R-32/125/134a inside a horizontal smooth tube Int. J. Heat Mass Transf. **2000**, 43 (19) 3651–3660.
[41] Stephan, K.; Abdelsalam, M. Heat transfer correlations for natural convection boiling Int. J. Heat Mass Transf. **1980,** 23 (1) 73–87.
[42] Pierre, B. Flow resistance with boiling refrigerants – Part 1 ASHRAE J. **1964,** 6 (9) 58-65.